1-1-2015

Geotechnics of granular materials for railways and port reclamation

Buddhima Indraratna
University of Wollongong, indra@uow.edu.au

Sanjay Nimbalkar
University of Wollongong, sanjayn@uow.edu.au

Ana Heitor
University of Wollongong, aheitor@uow.edu.au

Geotechnics of granular materials for railways and port reclamation

Abstract

Rail is one of the largest transportation modes offering freight and passenger traffic in rapidly developing nations, including India. Concerted efforts to improve productivity, modernization and technology upgrading have led to an impressive growth in railways and port infrastructure. Large-scale physical modelling and full-scale field monitoring often provide significant knowledge to better understand performance and to extend the current state-of-the-art in design of rail and port. A series of large-scale laboratory tests were conducted to analyse behaviour of granular materials (ballast, sub-ballast) under cyclic and impact loads. Effectiveness of using geosynthetic grids, geocells and shock mats was also studied. Comprehensive field trials were carried out on instrumented rail track sections and port reclamation sites in the towns of Bulli and Singleton and in Port Kembla (Wollongong), respectively. This keynote paper provides an insight to geotechnical behaviour of granular materials capturing the effects of degradation and deformation in railways and potential of using granular waste for the reclamation project in port.

Disciplines

Engineering | Science and Technology Studies

Publication Details

Indraratna, B., Nimbalkar, S. S. & Heitor, A. (2015). Geotechnics of granular materials for railways and port reclamation. 50th Indian Geotechnical Conference (pp. 1-18).

GEOTECHNICS OF GRANULAR MATERIALS FOR RAILWAYS AND PORT RECLAMATION

Buddhima Indraratna[1], Sanjay Nimbalkar[2], Ana Heitor[3]

ABSTRACT

Railroad is the largest transportation system offering freight and passenger traffic in rapidly developing nations, including India. Ports are important transportation hubs, forming the link between sea and land. These hubs must intelligently network various transportation systems so that people and goods can be transported in a safe, fast, efficient, and environmentally sound manner. Concerted efforts to improve productivity, modernization and technology upgrading have led to an impressive growth in railways and port infrastructure. Large-scale physical modeling and full-scale field monitoring often provide significant knowledge to better understand performance, and to extend the current state-of-the-art in design of rail and port.

As the axle loads and number of high-speed trains increase, the quality of track substructure becomes extremely important. The excessive deformation and degradation of the granular media (ballast, sub-ballast) under cyclic (repetitive) loading necessitates frequent track maintenance. Ballast and sub-ballast layers are designed to ensure that the cyclic loads are safely transmitted to the subgrade soils, and that the track is anchored transversely and longitudinally. But when these granular layers are not properly conditioned and confined, it is also one of the main sources of deteriorating track geometry. Discontinuity of the rail or wheel irregularities induces large impact loads which are detrimental to the track substructure. These impact loads are of very high magnitude and short duration depending on the nature of wheel or rail irregularities, and cause accelerated ballast breakage. To rectify these problems, the use of artificial inclusions such as geosynthetic grids and mats in the rail environment has been most effective (Fig. 1a). Comprehensive field trials were carried out to assess the role of geogrids, geocomposite, and shock mats in stabilising ballast embankments in the towns of Bulli and Singleton, New South Wales (NSW), Australia. Large-scale triaxial tests were conducted to investigate the behaviour of reinforced and unreinforced subballast under cyclic load using process simulation triaxial apparatus. Geocells influenced

[1]Professor of Civil Engineering and Research Director, Centre for Geomechanics and Railway Engineering, Faculty of Engineering and Information Sciences, University of Wollongong, Wollongong, Australia, indra@uow.edu.au

[2]Research Fellow, Centre for Geomechanics and Railway Engineering, Centre for Geomechanics and Railway Engineering, Faculty of Engineering and Information Sciences, University of Wollongong, Wollongong, Australia, sanjayn@uow.edu.au

[3]Lecturer, Centre for Geomechanics and Railway Engineering, Centre for Geomechanics and Railway Engineering, Faculty of Engineering and Information Sciences, University of Wollongong, Wollongong, Australia, aheitor@uow.edu.au

the behaviour of subballast under cyclic loading, particularly at low confining pressure and high frequency.

Waste minimisation and waste recycling are given a high priority in environmentally conscious industry today. Byproducts of the coal mining and steel industry including coal wash (CW) and steel furnace slag (SFS) are typically treated as wastes and disposed of in stockpiles occupying usable land. Innovative use of these granular wastes through civil engineering applications such as reclamation is vital for the local environment and economy. In this regard, an optimum CW-SFS mixture that may meet most of the geotechnical specifications is proposed based on a series of laboratory investigations. This proposed CW-SFS mixture was then used as fill for the reclamation project at the Outer Harbor extension of Port Kembla, at Wollongong, NSW (Fig. 1b). This keynote paper provides an insight to geotechnical behaviour of granular materials capturing the effects of degradation and deformation encountered in railways and potential of using granular waste for the reclamation project in port. Effective applications of geosynthetics, shock mats and geocells in railways are also described through results of large-scale laboratory testing and full-scale field monitoring.

Fig. 1 (a) Installation of geocomposite at Bulli (b) Compaction of granular waste at Port Kembla

Keywords: ballast, geosynthetics, shock mats, cyclic loads, impact forces, deformation, recycled materials.

GEOTECHNICS OF GRANULAR MATERIALS FOR RAILWAYS AND PORT RECLAMATION

B. Indraratna, Professor of Civil Engineering, University of Wollongong, Australia, email: indra@uow.edu.au
S. S. Nimbalkar, Research Fellow, University of Wollongong, Australia, email: sanjayn@uow.edu.au
A. Heitor, Lecturer, University of Wollongong, Australia, email: aheitor@uow.edu.au

ABSTRACT: Rail is one of the largest transportation modes offering freight and passenger traffic in rapidly developing nations, including India. Concerted efforts to improve productivity, modernization and technology upgrading have led to an impressive growth in railways and port infrastructure. Large-scale physical modelling and full-scale field monitoring often provide significant knowledge to better understand performance and to extend the current state-of-the-art in design of rail and port. A series of large-scale laboratory tests were conducted to analyse behaviour of granular materials (ballast, sub-ballast) under cyclic and impact loads. Effectiveness of using geosynthetic grids, geocells and shock mats was also studied. Comprehensive field trials were carried out on instrumented rail track sections and port reclamation sites in the towns of Bulli and Singleton and in Port Kembla (Wollongong), respectively. This keynote paper provides an insight to geotechnical behaviour of granular materials capturing the effects of degradation and deformation in railways and potential of using granular waste for the reclamation project in port.

INTRODUCTION

Railroad ballast layer is composed of graded layers of large and medium-sized crushed stone fragments placed below timber or concrete sleepers. It constitutes a major portion of track substructure ensuring that the cyclic (repeated) wheel loads are transmitted safely to the formation soils. The track structure is often subjected to high cyclic stresses under heavy freight and high-speed passenger trains. In recent times, differential track settlement owing to particle degradation and deformation of ballast layer under these high stresses has resulted into significantly high maintenance costs. In many countries including North America, Australia, China and India, a large proportion of funds allocated for the maintenance are usually spent on ballast replenishment.

The degradation of ballast layer is influenced by a number of factors including the magnitude (amplitude) of cyclic loading, the frequency and number of load cycles, the particle size distribution, the track (internal) confining pressure, and the size, shape as well as fracture toughness of individual aggregates [1-5]. For high load bearing capacity and maximum track stability, ballast needs to be angular, well graded, highly compacted [6-8], as well as reinforced with artificial inclusions [9-16]. The base reinforcement applications of two-dimensional (planar) geosynthetics (i.e. geogrid, geotextiles and geocomposite) in rail track have been studied in the past [17-22]. The effectiveness of geogrid reinforcement is highly dependent on the stiffness and size of the apertures [23,24]. The effectiveness of geotextile depends on its tensile membrane action [15]. The use of rubber shock mats to mitigate particle degradation in harsh track environment is appealing [4]. The use of geocells leads to improved performance of soil subjected to monotonic loading [25,26] and cyclic loading [27,28]. This improved performance is attributed to the apparent cohesion between geocell strips and infill material. In the recent past, three-dimensional

(cellular) geocells have found to be more effective at low track confinement [29,30].

Full-scale studies on instrumented tracks at Bulli (near Wollongong) and Singleton (near NewCastle) supported by Sydney Trains (formerly, RailCorp) and Australian Rail Track Corporation (ARTC), were carried out. In these studies, stresses and permanent track deformation were measured to evaluate the effectiveness of different types of geosynthetics and shock mats placed below the ballast, respectively [19-22].

Byproducts of coal mining and steel industries are coal wash (CW) and steel slag (BOS), respectively. These by-products are often disposed of in stockpiles which occupy usable land in urban areas. In view of the environment and the economy, these granular wastes should be recycled through appropriate large-scale civil engineering applications such as reclamation and/or backfill construction. However, due to the heterogeneity of these materials and their complex behavior, the design and construction utilizing these waste products poses significant geotechnical challenges especially under submerged conditions when used as reclamation fill in ports and harbors [31-33]. This keynote paper describes the results of large-scale laboratory tests as well as full-scale field studies in railways and port reclamation works.

GEOTECHNICAL BEHAVIOUR OF BALLAST

Ballast is usually composed of blasted (quarried) rock aggregates originating from high quality igneous or metamorphic rock quarries and usually includes dolomite, rheolite, gneiss, basalt, granite, and quartzite [34]. It is composed of medium to coarse gravel sized aggregates (10 - 60 mm).

Ballast Degradation

The ballast degradation is a complex mechanism that usually initiates with the breakage of asperities (sharp corners/projections), followed by complete crushing of weaker particles under further loading. A new Ballast Breakage Index (BBI) is proposed specifically for railway ballast to quantify the extent of degradation [2]. It is based on the particle size distribution (PSD) curves. The ballast breakage index (BBI) is calculated on the basis of changes in the fraction passing a range of sieves, as shown in Fig. 1.

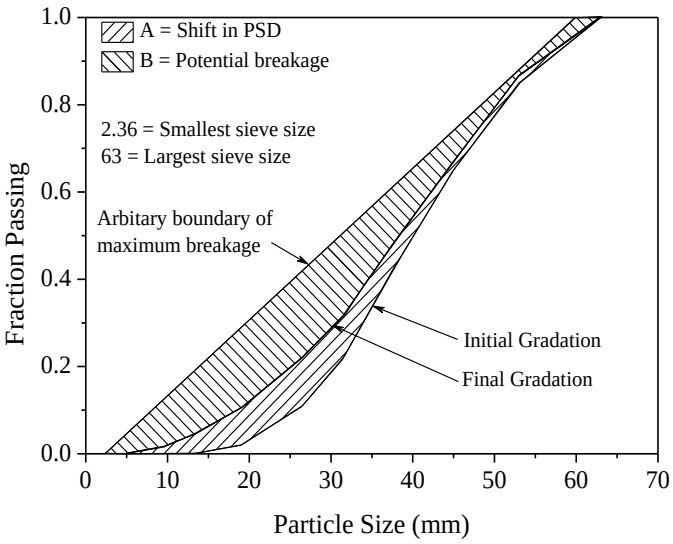

Fig. 1 Ballast breakage index (BBI) calculation method (data sourced from Indraratna et al. [2]).

The increase in extent of particle breakage causes the PSD curve to shift further towards the smaller particles size region on a conventional PSD plot. An increase in the area A between the initial and final PSD results in a greater BBI value. BBI has a lower limit of 0 and an upper limit of 1. By referring to the linear particle size axis, BBI can be calculated by using ratio of A/(A+B), where A is the area defined previously, and B is the potential breakage or area between the arbitrary boundary of maximum breakage and the final particle size distribution.

Constitutive Modelling of Ballast

A continuum mechanics-based constitutive model incorporating dilatancy and plastic flow rule was developed to capture breakage of coarse aggregates which can be applied to railway ballast [35]. The model was based on the critical state concept and the theory of plasticity with a kinematic-type yield locus (constant stress ratio). The theoretical formulation relates the deviator stress ratio at any stage of shearing with the basic friction angle, dilation rate and the energy consumption due to particle breakage. The increments of plastic

distortional and volumetric strains are given by [35]:

$$d\varepsilon_s^p = \frac{2\alpha\kappa\left(\frac{p}{p_{cs}}\right)\left(1-\frac{p_{o(i)}}{p_{cs(i)}}\right)\left(9+3M-2\eta^* M\right)\eta d\eta}{9M^2\left(1+e_i\right)\left(\frac{2p_o}{p}-1\right)\left(M-\eta^*\right)} \quad (1)$$

$$\frac{d\varepsilon_v^p}{d\varepsilon_s^p} = \frac{9(M-\eta)}{9+3M-2\eta^* M} + \frac{\beta dB_g}{pd\varepsilon_s^p}\left(\frac{9-3M}{9+3M-2\eta^* M}\right)\left(\frac{6+4M}{6+M}\right) \quad (2)$$

where, $d\varepsilon_s^p$ and $d\varepsilon_v^p$ are the increments of plastic distortional and volumetric strain, respectively. The parameter p is the effective mean stress and p_{cs} is the value of p on the critical state line at the current void ratio. The subscript i indicates the initial value at the start of shearing. The parameter, η is the stress ratio ($=q/p$), q is the deviator stress, $\eta^* = \eta\,(p/p_{cs})$, M is the critical state stress ratio, e_i is the initial void ratio, κ is the negative slope of compression curve (e-lnp). α and B are dimensionless constants. χ and μ are the material constants defining the rate of ballast breakage.

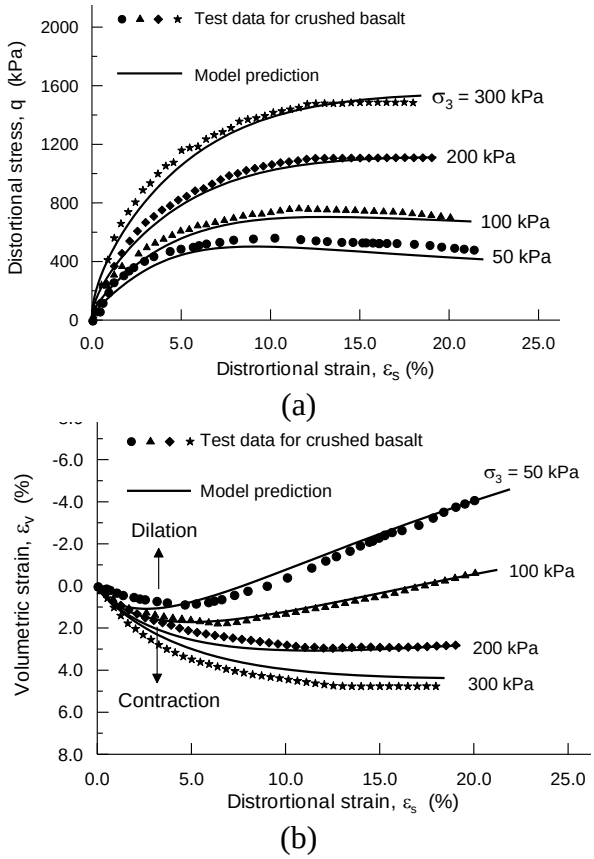

Fig. 2 Model predictions for (a) stress-strain and (b) volume change behavior (data sourced from Salim and Indraratna [35])

This model was verified using large-scale triaxial laboratory results (Fig. 2). The above constitutive model contained 11 parameters, which could be evaluated using drained triaxial test results alongside the particle breakage measurements.

Effect of Confining Pressure

The ballast degradation under cyclic loading can be categorised into three distinct zones [3]. These zones are defined on the basis of range of confining pressure (σ'_3) as: the Dilatant Unstable Degradation Zone (DUDZ) for σ'_3 < 30 kPa), the Optimum Degradation Zone (ODZ) for σ'_3 = 30 - 75 kPa), and the Compressive Stable Degradation Zone (CSDZ) for σ'_3 > 75 kPa), as shown in Fig. 3.

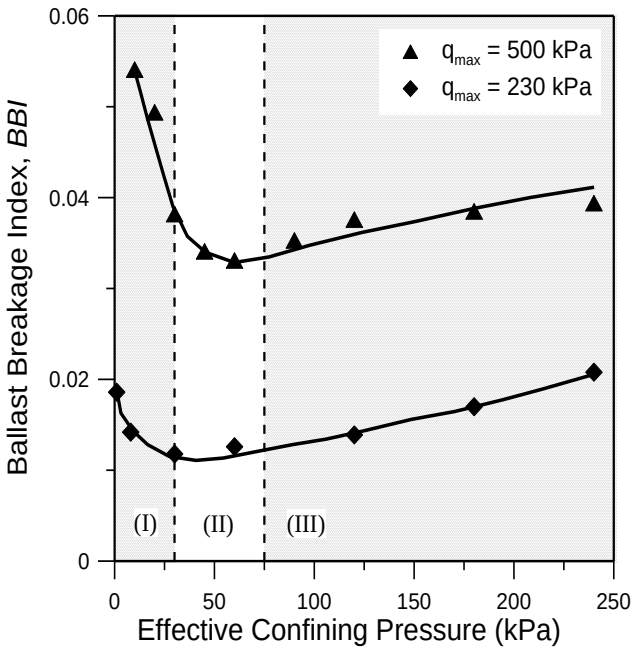

Fig. 3 Effect of confining pressure on particle degradation (data sourced from Indraratna et al. [2]).

In the DUDZ zone, ballast specimens are characterised by limited particle-to-particle contact areas and undergo considerable degradation as a result of shearing and attrition of angular projections. In the ODZ region, the particles are held together with enough lateral confinement to provide increased inter-particle contact areas, which in turn reduces the risk of breakage. At higher σ'_3 (CSDZ region), the particles are forced against each other, which limits any sliding or rolling, and therefore breakage is significantly

increased. Due to the large lateral forces being applied to the samples in this region, volumetric compression is enhanced, which is partly due to an increase in particle breakage.

STABILISING BALLASTED TRACK USING GEOCELLS: PROCESS SIMULATION APPARATUS

A series of drained triaxial tests were conducted using the Process Simulation Prismoidal Triaxial Apparatus (PSPTA) as shown in Fig. 4. This large-scale apparatus (800 mm in length, 600 mm in width and 600 mm in height) was large enough to accommodate a unit cell, the size of which was chosen to represent the effective sleeper length (l = 800 mm) and the sleeper spacing (s = 600 mm) [30]. The effective sleeper length is assumed to be one-third of the total sleeper length (L = 2400 mm) [36]. Thus, the test results presented herewith does not suffer from reduced scale effect.

Fig. 4 Process Simulation Prismoidal Triaxial Apparatus (PSPTA) designed and built at University of Wollongong.

The particle size distribution of subballast was in accordance with Australian standards (D_{max} = 19 mm, D_{min} = 0.075 mm, D_{50} = 3.3 mm, C_u = 16.3 and C_c = 1.3). Geocell used in this study was made from polyethylene material with elliptical shape. In order to investigate the behaviour of both unreinforced and geocell reinforced sub-ballast, cyclic loading tests were conducted at different confining pressures (σ'_3 = 5, 10, 15, 20 and 30 kPa) and frequencies (f = 10, 20 and 30 Hz) using stress controlled mode. The required cyclic loading magnitude (maximum deviator stress, q_{max} = 166 kPa and minimum deviator stress, q_{min} =41 kPa) was calculated based on 30 tonnes axle load used in NSW heavy haul. A plane strain condition (ε_2=0) was simulated by preventing lateral movement in direction of intermediate principal stress (σ'_2), perpendicular to the direction of sleeper. All experiments were conducted up to number of cycles (N) of 500,000 cycles.

Results and Discussion

Vertical Deformation

Figure 5 shows the variation of vertical deformation (S_V) of unreinforced and geocell reinforced sub-ballast against confining pressures.

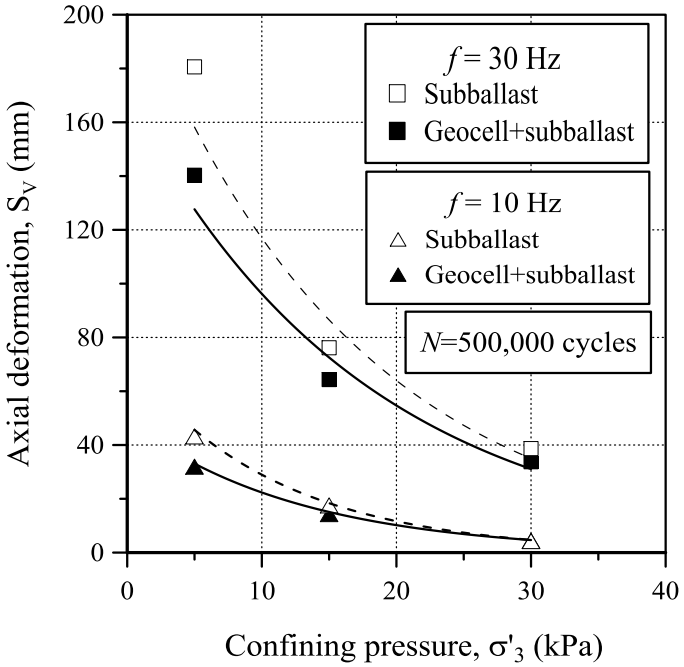

Fig. 5 Effect of confining pressure on vertical deformation of unreinforced and reinforced sub-ballast (data sourced from Indraratna et al. [30], with permission from ASCE)

At σ'_3 < 20 kPa, sub-ballast undergoes significant particle rearrangement and densification leading to excessive settlement. The magnitude of S_V was largest (about 180 mm) at higher frequencies (f >10

Hz) and lower confining pressures. Nevertheless, employing of the geocell in the specimen caused substantial reduction of S_V in reinforced specimen of about 22%. This is because, most of the cyclic stress is attenuated by the geocell mattress, and reduced stress is transferred to the lower layer. The results also showed that the magnitude of vertical settlement was significantly diminished at higher confining pressure. By comparing experimental results of lateral spreading (S_L) and vertical settlement (S_V), it is stated that unreinforced and geocell reinforced sub-ballast exhibited similar behaviour at the confining pressure (σ'_3) of 30 kPa. This indicates that geocell has less influence on the specimen behaviour with higher confining pressure. As a result, σ'_3 = 30 kPa can be selected as an optimum confining pressure to reduced excessive lateral spreading of sub-ballast.

Lateral Deformation

The most beneficial impact of using the geocell mattress is minimising lateral (S_L) and vertical (S_V) deformation of sub-ballast at the end of cyclic loading phase (i.e. N = 500,000). Figure 6 shows the lateral deformation of unreinforced and geocell reinforced sub-ballast.

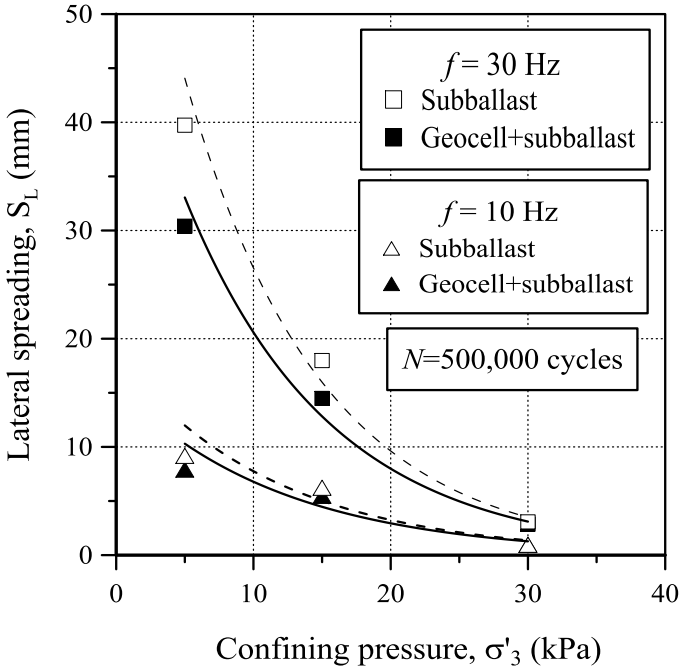

Fig. 6 Effect of confining pressure on lateral deformation of unreinforced and reinforced sub-ballast (data sourced from Indraratna et al. [30], with permission from ASCE)

As shown in Fig. 6, sub-ballast experienced significant lateral spreading at very low confining pressures (σ'_3 < 20 kPa) when used without geocell mattress. The magnitude of S_L was reduced by increasing confining pressures (σ'_3). However, the results showed that the degree of lateral deformation was remarkable reduced upon using geocell mattress in the sub-ballast. This is because geocell confines infill aggregate and creates a self-stabilizing ring, hence arrest excessive lateral spreading. The maximum reduction of 20 % in S_L due to use of the geocell mattress was observed at σ'_3 < 20 kPa. This can be justified because at very low σ'_3, there will be higher tensile strength mobilized in the geocell, under cyclic loading. Marginal improvement was observed in reinforced specimens, at higher confining pressures (i.e., $\sigma'_3 \geq$ 20 kPa).

Also, it was found that the behaviour of granular medium was significantly influenced by the applied cyclic load frequency, as shown in Fig. 6. The magnitude of lateral spreading was markedly increased (S_L = 40 mm) by increasing frequency f =10-30 Hz. However, the geocell was successfully applied to improve specimen performance by diminishing the impact of the frequency of cyclic loading in reinforced specimens. The effect of geocell reinforcement was found to be more profound at higher frequency testing. The results also indicated that at lower frequency (f) the specimens were not influenced as mush, even at lower confining pressures. This is because higher tensile strength will be mobilized at higher frequencies, lead to highlight the impact of geocell mattress.

Resilient Modulus

Another important parameter that was found to be influenced by the geocell reinforcement, is resilient modulus (M_R). The values of resilient modulus are plotted at different confining pressures in Fig. 7.

By increasing the confining pressure, the magnitude of M_R was increased. This is because granular materials undergo extensive densification, leading to an enhanced resilient modulus.

Nevertheless, in the reinforced specimen, the degree of improvement was observed to be higher than reinforced specimen. This is due to the fact that in reinforced specimen, by confining infill material, the geocell mattress acts as a semi-rigid mattress, with higher stiffness.

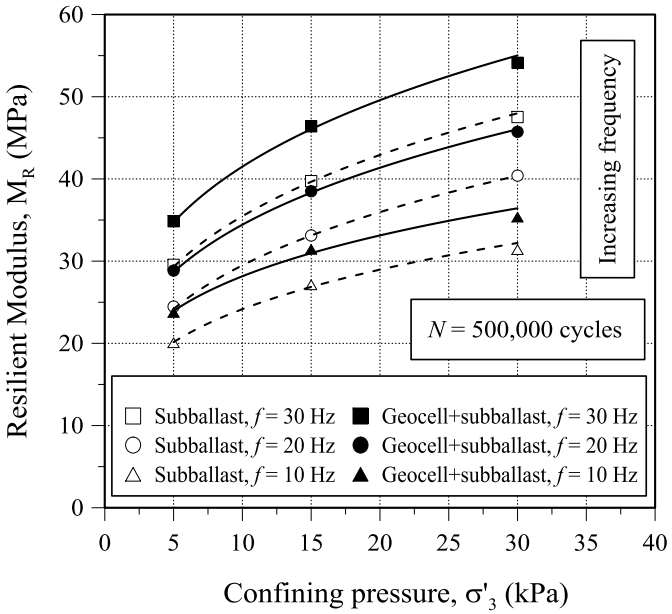

Fig. 7 Variation of resilient modulus at different confining pressures (σ'_3) for unreinforced and reinforced sub-ballast (data sourced from Indraratna et al. [30], with permission from ASCE)

STABILISING BALLASTED TRACK USING GEOGRIDS: PROCESS SIMULATION APPARATUS

A series of drained triaxial tests were conducted using the Process Simulation Prismoidal Triaxial Apparatus (PSPTA) as shown in Fig. 4. A strain-controlled load was applied initially at a rate of 1 mm/s until the mean level of cyclic deviator stress was attained. A vertical cyclic load was then applied by a servo-dynamic hydraulic actuator with a maximum cyclic stress ($\sigma'_{1,max,cyc}$) of 447 kPa. A frequency of 15 Hz was considered appropriate to simulate a train travelling at approximately 110 km/h. The maximum cyclic stress was determined using the American Railway Engineering Association (AREA) method [14]. The confining pressure was applied on the sides of the apparatus by the hydraulic jacks. The initial lateral confining pressures (σ'_3) of 7 kPa in the transverse direction (parallel to sleeper), and (σ'_2) of 10 kPa along the longitudinal direction (parallel to rail) were applied. Cyclic vertical stresses were measured using pressure cells (diameter 230 mm, thickness 12 mm) installed at the sleeper-ballast and ballast-subballast interfaces. The settlement pegs and linear voltage differential transformers (LVDTs) were installed in order to record vertical as well as lateral deformations, respectively. The settlement pegs consisted of 100 mm size square base plates attached to 10 mm diameter circular rods.

The ballast and subballast material was procured from a locally available quarry near Wollongong City, Australia. The fresh ballast consisted of 300 mm thick layer and it was underlain by 100 mm thick subballast. The bottom most 50 mm thick layer consisted of clayey sand. The ballast and subballast was compacted to achieve bulk densities of 1560 kg/m^3 and 2426 kg/m^3, respectively. These layers were compacted to ensure representative field densities. A single layer of planar geosynthetics was placed below the ballast layer. All tests were conducted up to number of cycles (N) of 200000. No damage on the geogrid or geotextile was evident after the testing.

Results and Discussion

The cyclic loading performance of ballast layer was evaluated in terms of vertical and lateral strains. The unreinforced as well as reinforced cases were analyzed in view of strain control. The results are summarized below.

Vertical Strain

The vertical deformation of ballast was determined by excluding the deformation of the underlying layers (subballast and subgrade) from overall track deformation. The strain was then determined by considering the change of deformation over the initial layer thickness. It is pertinent to note that these strains were measured using settlement pegs and were irrecoverable (or fully plastic). Under the application of cyclic load, the ballast specimen underwent compression in the vertical direction [vertical strain (ε_v)] and expanded in the lateral directions [lateral strains (ε_2, ε_3), where ε_2 is measured in a direction parallel to rail, and ε_3 is

measured in a direction parallel to sleeper]. Figure 8(a) shows a variation in the vertical strain (ε_1) of ballast against an increasing number of load cycles. As anticipated, the ballast deformed rapidly when the loading cycles commenced, although its rate of deformation diminished to a 'stable' phase after reaching a certain number of load cycles. The ballast materials showed a strong tendency to compact under high frequency cyclic loading. Reorientation and rearrangement of aggregates coupled with significant breakage leads to a denser (compressive) packing assembly. This is in agreement with findings reported elsewhere [37,38].

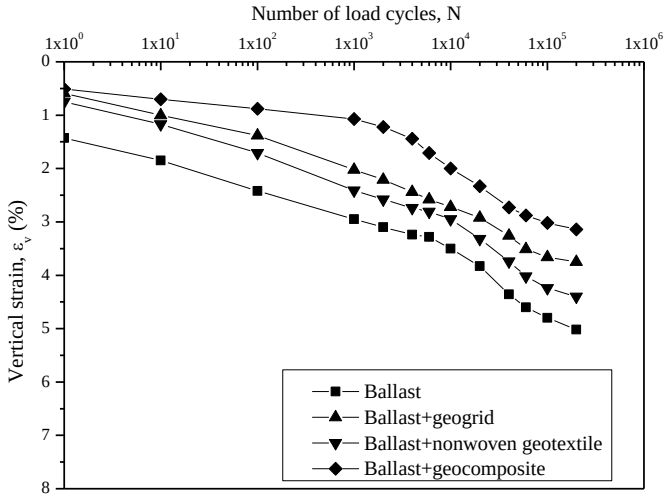

Fig. 8(a) Variation of vertical strain (ε_v) with number of load cycles (N) (data sourced from Indraratna & Nimbalkar [15]).

The vertical deformation (or strain) is characterized by three phases. The first phase is the immediate deformation under the first loading cycle. The second phase can be termed as 'unstable' during which rapid deformation occurs. In the third phase, the rate of increase of deformation is marginal thus characterizing 'stable shakedown' behavior [15,39]. The ballast underlain by geosynthetics exhibited a lower vertical strain than unreinforced counterpart (Fig. 8a). The geogrid was found to be more effective than the non-woven geotextile. This is because, the former could develop strong frictional interlock with highly angular aggregates of ballast layer. The fresh ballast stabilized using the geocomposite (a combination of geogrid and geotextile) exhibited the least vertical deformation.

Lateral Strain

Figure 8(b) shows lateral strain (ε_h) of ballast layer plotted against increasing number of load cycles. The geogrid decreased the lateral strain of the ballast substantially compared to the non-woven geotextile. The geogrid provided internal confinement thus improved lateral stability. The reinforcement action of the geogrid is generated during cyclic loading, and it is responsible for the reduction in lateral deformations of the ballast [12]. Furthermore, use of geocomposite controlled the lateral strain most effectively as shown in Fig. 8(b). This result has significant implications in view of the potential benefits of these artificial inclusions in the improvement of lateral stability of ballast embankments.

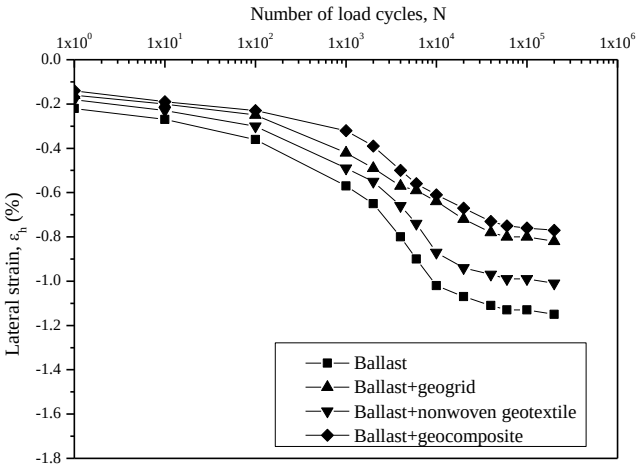

Fig. 8(b) Variation of lateral strain (ε_h) with number of load cycles (N) (data sourced from Indraratna & Nimbalkar [15]).

STABILISING BALLASTED TRACK USING GEOGRIDS: MODIFIED PROCESS SIMULATION APPARATUS

In order to capture the non-linear variation of lateral deformations with depth, the Modified Process Simulation Prismoidal Triaxial Apparatus (MPSPTA) was used. The modification involved the replacement of the side wall with a wall containing five movable plates each of 64 mm in height [16]. Cyclic tests were carried out at a frequency of 20 Hz which corresponds to a train speed of about 150 km/h using the method explained in previous section. The geogrids were

selected based on the interface efficiency factor (α), obtained from direct shear tests and these details are given elsewhere [24]. A vertical maximum cyclic stress ($\sigma'_{1,max,cyc}$) of 460 kPa corresponding to an axle load of 225 kN was applied. A confining pressure (σ'_3) of 10 kPa was applied to the modified side wall.

Lateral Spread Reduction Index (LSRI)

The improved performance of geogrid-reinforced ballast can be evaluated in terms of a normalized parameter called lateral spread reduction index (LSRI). It is defined as [15]:

$$LSRI = \frac{S_{l(unreinforced)} - S_{l(reinforced)}}{S_{l(unreinforced)}} \quad (3)$$

where, $S_{l(unreinforced)}$ and $S_{l(reinforced)}$ are lateral deformations of unreinforced and reinforced ballast, respectively. LSRI of zero indicates unreinforced condition whereas a value of unity represents no particle spreading. On the other hand, a negative value of LSRI indicates an increase in lateral deformation due to the inclusion of reinforcement.

Effects of A/D_{50} on LSRI

Figure 9 shows the variation of average LSRI along the depth with the ratio A/D_{50}, for both the geogrid placement positions (i.e. at z = 0 and 65 mm). The values of A/D_{50} for different geogrids were adapted from Indraratna et al. [24], wherein the A/D_{50} of geogrid 'G2' was based on the diameter of the largest circle inscribed within the triangular aperture.

It was noted that for geogrid placed below ballast, the average LSRI increases significantly from 0.06 to 0.25 as A/D_{50} increases from 0.6 to 1.20. This may be attributed to the better geogrid-particle interlock attained as the geogrid aperture size increases for a given ballast size. The geogrid 'G4' with A/D_{50} of 1.21 gives a maximum LSRI of 0.25. However, with the further increase in A/D_{50} from 1.21 to 1.85 the average LSRI decreases from 0.25 to 0.20. For the geogrid placed at 65 mm above the subballast, the average LSRI follows an almost similar trend with A/D_{50} except that the geogrid 'G2' exhibits a negative LSRI.

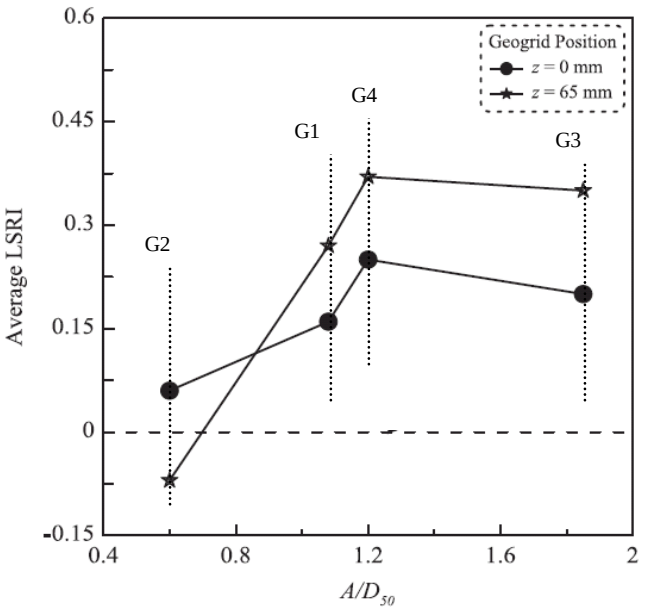

Fig. 9 Variation of average LSRI with A/D_{50} (data sourced from Indraratna et al. [16]).

Effects of LSRI on Deformation and BBI

It was observed that as the average LSRI increases, both the deformation and the particle breakage decrease significantly. The deformation and BBI decrease from about 23.5 to 9.8 mm and 9.89 to 4.6%, respectively, as the average LSRI increases from zero to 0.37. A linear increase in deformation was observed with the increase in BBI as given by [16]:

$$S_{v(reinforced)} = 0.0243BBI - 1.74 \quad (4)$$

Equation (4) also highlights that the particle breakage also contributed to a significant portion of deformation.

FIELD STUDY: BULLI TOWN

In order to assess the effects of using planar geosynthetics in fresh and recycled ballast, a field study was undertaken at Bulli in the State of NSW [18,19].

Track Construction

The proposed location for track construction was selected between two turnouts at Bulli, along the south coast of NSW. The instrumented track was divided into four 15 m long sections. The ballast and subballast were 300 mm and 150 mm in thickness, respectively. A single layer of

geocomposite was used below the fresh and recycled ballast (Fig. 10).

Fig. 10 Installation of geocomposite at Bulli.

The particle size distributions of various materials and technical specifications of geosynthetics are given in Indraratna *et al*. [19].

Track Instrumentation

Various types of sophisticated instruments were used for measuring in-situ track performance. The vertical and horizontal stresses were measured by pressure cells. Vertical and lateral deformations were measured by settlement pegs and displacement transducers, respectively (Fig. 11).

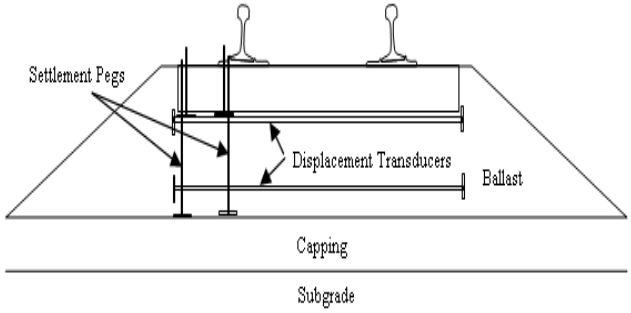

Fig. 11 Installation of settlement pegs and displacement transducers (data sourced from Indraratna et al. [38], with permission from ASCE).

Track Measurements

Peak Stresses in Ballast

Figure 12 shows the vertical and lateral maximum cyclic stresses (σ'_v,σ'_h) measured due to passage of train travelling at 60 km/h. The large vertical stresses and relatively small lateral stresses caused large shear strains in the ballast.

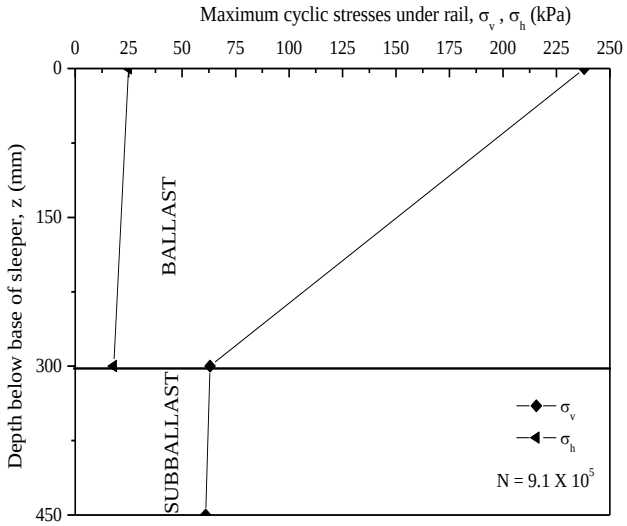

Fig. 12 Vertical and lateral maximum cyclic stresses (σ'_v, σ'_h) (data sourced from Indraratna et al. [19], with permission from ASCE).

Lateral Deformations

The lateral deformations were determined from the mean of measurements between the sleeper and ballast, and between the ballast and subballast. The lateral deformations are plotted against the number of load cycles (N) in Fig. 13. The recycled ballast exhibited less vertical and lateral deformations. This is because, its particle size distribution (C_u = 1.8) was moderately graded compared to very uniform fresh ballast (C_u = 1.5).

The apertures of the geocomposite offered a strong mechanical interlock with ballast aggregates, forming a highly frictional interface. The capacity of the ballast to distribute stresses was improved by the use of the geosynthetic layer, which also resulted into substantially reduced deformation.

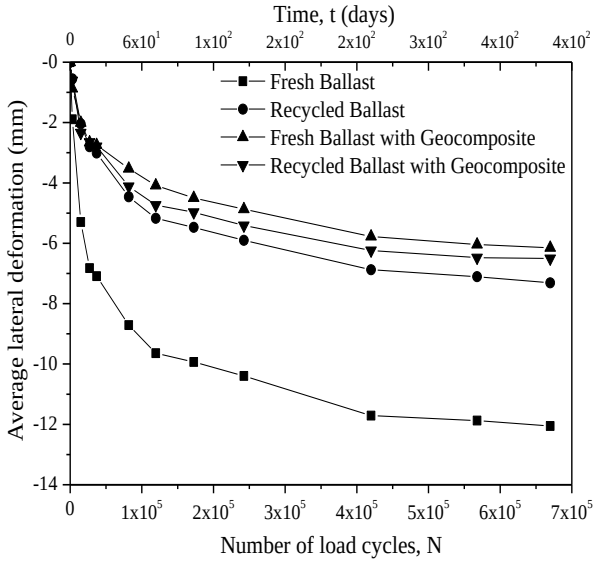

Fig. 13 Lateral deformations of the ballast (data sourced from Indraratna et al. [19], with permission from ASCE).

USE OF SHOCK MATS FOR MITIGATING BALLAST BREAKAGE INDUCED BY IMPACT

A series of laboratory tests were carried out to evaluate the effectiveness of shock mats in the attenuation of high frequency impact loads and subsequent mitigation of ballast deformations and degradation. Large scale drop-weight impact testing equipment was used for this study as shown in Fig. 14. The impact testing equipment consists of a free-fall hammer of 5.81 kN weight that can be dropped from a maximum height of 6 m with an equivalent maximum drop velocity of 10 m/s.

In order to eliminate surrounding noise and ground motion, an isolated concrete foundation (5.0 m × 3.0 m × 2.5 m) was designed to bear a significantly higher fundamental frequency than the test apparatus. The particle size distribution of ballast specimens was prepared in accordance with the current practice in Australia [39]. A thin layer of compacted sand was used in the laboratory physical model to simulate a typical 'weak' subgrade. The 10 mm thick shock mat used in the study was made of recycled rubber granulates of 1-3 mm size particles, bound by polyurethane elastomer compound (tensile strength = 600 kN/m^2, Modulus at 10% compressive strain = 3800 kN/m^2).

Fig. 14 Drop weight impact testing equipment.

Test procedure

The ballast was thoroughly cleaned, dried, sieved through a set of standard sieves (aperture size 53: 13.2 mm). The ballast specimens (C_u = 1.6, C_c = 1.0, and d_{50} = 35 mm) were compacted in several layers to simulate the field densities of heavy haul tracks. In order to resemble low track confining pressure in the field, test specimens were confined in a rubber membrane. A steel plate (t = 50 mm) was used to represent a hard base. In order to simulate relatively weak subgrade conditions, a 100 mm thick, vibro-compacted sand cushion was placed below the ballast bed. Three layers of shock mat accounting to a total thickness of 30 mm were used. The drop hammer was raised mechanically to the required height and then released by an electronic quick release system. The impact load was stopped after 10 blows due to an attenuation of strains in the ballast layer.

Ballast Breakage

After each test, the ballast sample was sieved to obtain BBI. The BBI values are presented in Table 1. The higher breakage of ballast particles can be attributed to the considerable non-uniform stress concentrations occurring at the corners of the sharp angular particles. The application of just 10 impact blows caused considerable ballast breakage (i.e. BBI = 17%) when a stiff subgrade was used but when a shock mat was placed above and below the ballast bed, particle breakage was reduced by approximately 47% for a stiff subgrade and about 65% for a relatively weak subgrade.

Table 1 Ballast breakage under impact loads [41].

Test No.	Base type	Shock Mat Details	*BBI*
1	Stiff	Without shock mat	0.170
2	Stiff	Shock mat at top and bottom	0.091
3	Weak	Without shock mat	0.080
4	Weak	Shock mat at top and bottom	0.028

FIELD STUDY: SINGLETON TOWN

To investigate the 'in-situ' performance of different types of geosynthetics, an extensive study was undertaken on an instrumented track near Singleton, NSW [21].

Track Construction

The instrumented track was divided into eight 200 m long sections. These sections were built on three different types of sub-grades, including the soft alluvial silty clay deposit, the hard rock, and the concrete bridge deck. A layer of geosynthetics was placed below the fresh ballast. The details of track construction and material specifications can be found in Indraratna et al. [21].

Track Instrumentation

Different types of sensors were used. Strain gauges were used to measure mobilized strains in geogrids. Traffic induced vertical stresses were monitored by pressure cells. Settlement pegs were installed to measure vertical deformations of the ballast in the similar fashion as discussed in previous section.

Track Measurements

Traffic Induced Vertical Stresses

The vertical stress below ballast (σ'_v) due to the passage of train with an axle load of 30 tonnes travelling at about 40 km/h was about 280 kPa at the bridge deck. This stress was about 35 kPa at soft alluvial deposit. Vertical stress below sleeper at the hard rock was 180 kPa. This indicated that the traffic-induced stresses were considerably larger in the track with a stiffer subgrade.

Vertical Deformations

The ballast deformations (S_v) are plotted against the number of load cycles (N), as shown in Fig. 15 (a & b). These results indicated that the non-linear variation of ballast deformations. The rate at which the deformations increased actually decreased as the number of load cycles increased.

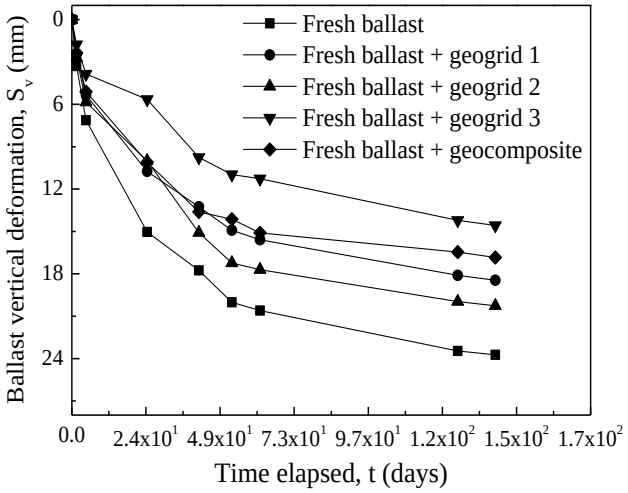

Fig. 15(a) Vertical deformations of ballast layer for soft alluvial deposit (data sourced from Indraratna et al., [42]).

The vertical deformations of the ballast reinforced with geogrids were 10-32% smaller than those without reinforcement. This pattern was similar to that observed in the laboratory [11,15,43], and was mainly attributed to the interlocking between the ballast particles and grids. It was also apparent that the ability of geogrid reinforcement to reduce ballast deformation was generally higher for softer subgrades. The larger deformations also caused significant particle breakage, as discussed below.

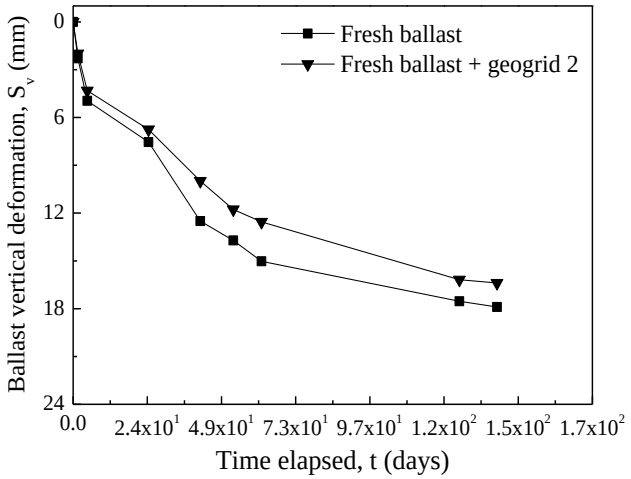

Fig. 15(b) Vertical deformations of ballast layer for hard rock (data sourced from Indraratna et al., [42]).

Ballast Breakage

The ballast breakage index (BBI) after N = 750,000 load cycles for bridge deck was 17%, while soft deposit and hard rock were 9.8% and 13.1%, respectively. The reduced breakage is due to additional confinement [44] offered by the barriers of the Mudies Creek bridge. These results also suggest the effectiveness of shock mats in reducing particle degradation when placed above the concrete deck.

PORT RECLAMATION WITH COAL WASH AND STEEL SLAG FINES

The 45 ha reclamation project involves the Outer Harbor extension of Port Kembla, Wollongong, NSW. Its layout is shown in Fig. 16. Coal wash (CW) and basic oxygen steel slag fines (BOS) are by-products of the coal mining and steel industries, respectively.

In this project, the assessment of the potential for using CW and BOS as an alternative to the conventional freshly quarried or dredged sand fills was necessary. In this regard, detailed laboratory investigations were conducted at the University of Wollongong. The results suggested an optimum CW-BOS mixtures that may meet most of the geotechnical specifications and therefore could be used as an effective structural fill. Their use as a suitable reclamation fill would be good for at least the compacted bunds above the high tide level.

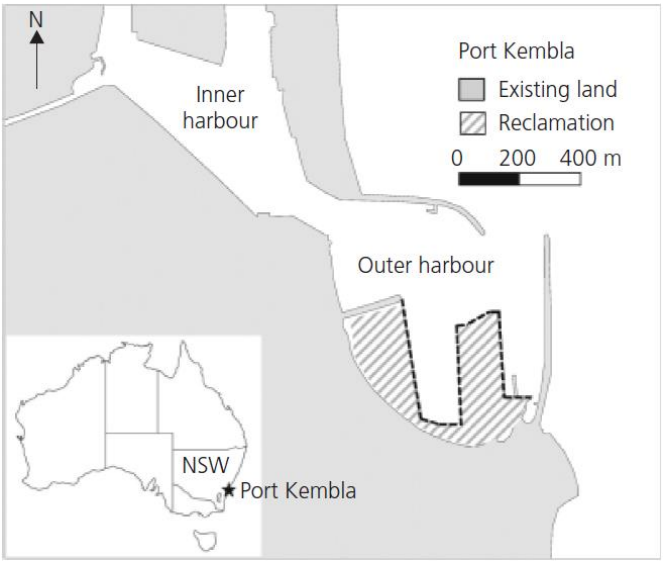

Fig. 16 Layout of Port Kembla expansion project [45].

Geotechnical Characterization of Blended Waste Materials

Determining the geotechnical characteristics is crucial for assessing the suitability of industrial granular wastes as construction fills [31-33]. By the Unified Soil Classification System, typical CW and BOS samples (fill material) could be categorized as well-graded gravel (GW) and well-graded sand (SW), respectively. The laboratory samples are shown in Fig. 17.

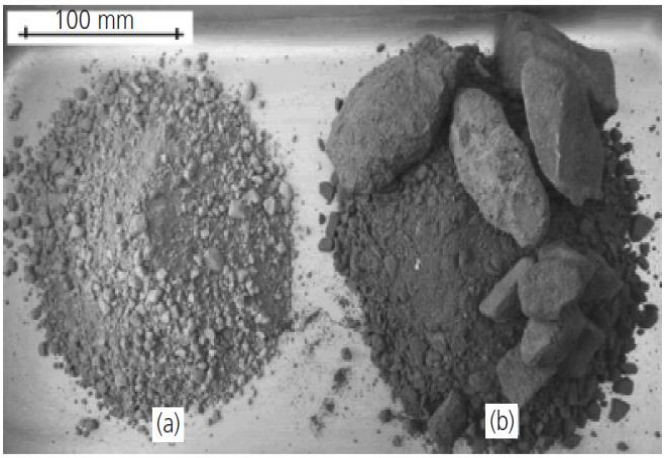

Fig. 17 Typical samples of (a) BOS and (b) CW [46].

Since the entire range of particle size distribution could not be used for laboratory testing, only the sandy fraction was tested as shown in Fig. 18. The

average specific gravity (G_s) of the CW and SFS samples was 2.13 and 3.48, respectively. The lower G_s value of CW was caused by the presence of coal, while the higher G_s value of BOS was attributed to the presence of iron. Compared to conventional (quartz-dominant) fill materials (G_s = 2.6-2.7), CW is a lighter material, while BOS is heavier.

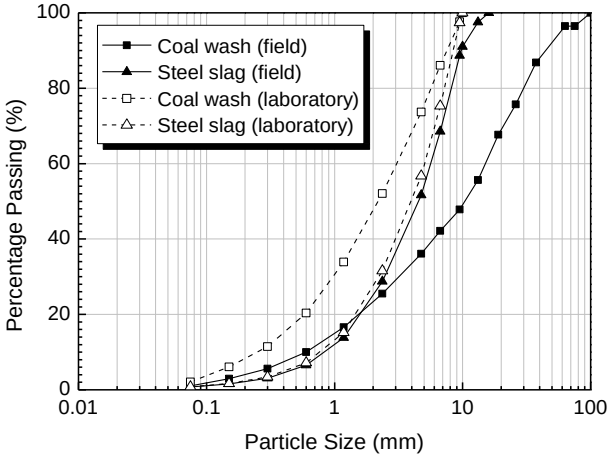

Fig. 18 Particle size distribution of CW and BOS [45].

Laboratory Tests

Compaction

The standard Proctor compaction tests (Fig. 19) showed that when the BOS content increased from 0% to 100%, the maximum dry density increased from 15 kN/m^3 to 22 kN/m^3, and the optimum water content decreased slightly from 10.8% to 9.5%. Such a remarkable variation in maximum dry density is essentially governed by the significant increase of G_s for mixtures from 2.13 to 3.48. The maximum dry density of mixtures with 40-60% of SFS were comparable to the maximum dry density of most compacted sandy fills (18 kN/m^3).

Permeability

Different mixtures were compacted at their optimum moisture content, and then constant head permeability tests were conducted on them with standard compaction energy. Figure 20 shows as the percentage of CW increased from 0% to 100% the permeability decreased from 3 × 10^{-3} cm/s (similar to gravel fills) to 2 × 10^{-7} cm/s (similar to clayey fills). Instead, the permeability coefficients of blended specimens which contain 40-60% of CW were comparable to those of most compacted sandy fills (1 × 10^{-5} cm/s).

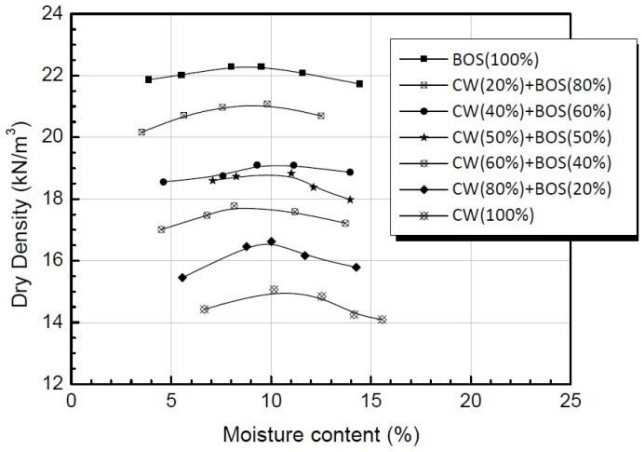

Fig. 19 Standard Proctor compaction tests [45].

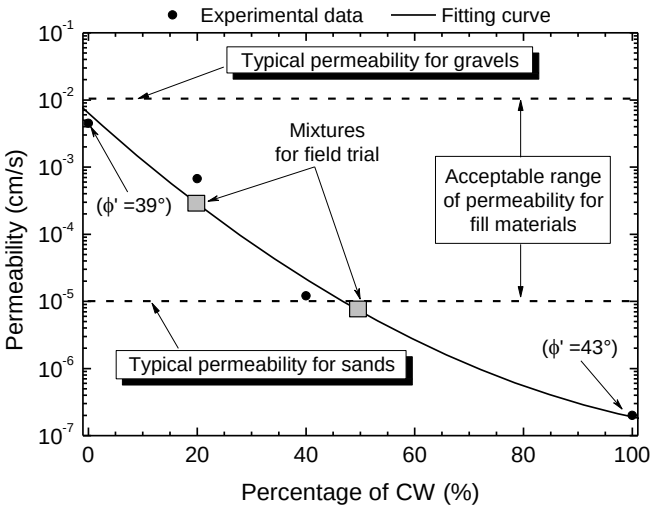

Fig. 20 Variation of permeability with coal wash percentage and friction angle [45].

Shear Strength

The shear strength of CW and BOS was investigated using consolidated drained compression triaxial tests. The specimens were prepared with a density exceeding 95% of maximum dry density and sheared at a strain rate of 0.2 mm/min. The friction angles (ϕ') of CW and BOS were tested to be from 39° to 44°, which were somewhat greater than what is typically expected from conventional fills (> 30°).

Acceptance Criteria for Granular Waste Fills

In order to optimize the use of waste materials in reclamation, the following criteria for the permeability and strength of conventional fills may generally be considered:

(i) Placed fill material should possess a higher friction angle ($\phi \geq 30°$); and

(ii) Placed fill material should have a higher permeability coefficient ($1 \times 10^{-6} < k < 1 \times 10^{-4}$ cm/s), to guarantee rapid dissipation of excess pore pressure, as well as to minimize internal erosion or suffusion. A modified framework with comprehensive design criteria including foul levers of acceptance is proposed [46] and is shown in Fig. 21.

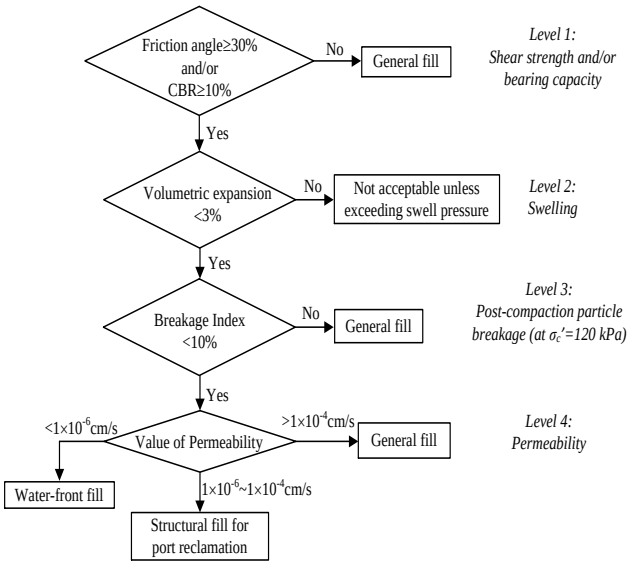

Fig. 21 Optimization of CW-BOS blend as structural fill material for port reclamation [46].

Waste Fill Design and Field Trial Tests

To satisfy the above stated design criteria, the blended waste mixtures should have a content of CW > 50%. The actual performance of a compacted fill in the field can be quite different from that observed in the laboratory for much smaller specimens with reduced gradations enclosed within a rigid boundary of the compaction chambers. As a result, it was important to validate the laboratory findings with the actual field behavior of CW-SFS mixtures and establish the most appropriate compaction method and associated machinery.

For this purpose, field trial tests were carried out at Port Kembla reclamation site to evaluate the performance of two selected CW-SFS mixtures and to establish an appropriate compaction method for CW-SFS fills. Nevertheless, the field trial was an essential part of this investigation to properly assess *in-situ* swelling and to recognize the advantages and limitations of blended mixtures as compacted fill material. A pit with dimensions of 55 m long, 14 m wide and 1.4 m deep was provided for the field trial (Fig. 22).

Fig. 22 Port Kembla construction site: prior fill placement [45].

The area was divided into two equal subsections having a volume of 540 m^3 and filled by CW-SFS 50/50 by volume and CW-SFS 33/67 by volume. Approximately 1200 tonnes of CW and 1600 tonnes of SFS were used. Compaction of 300-mm thick layers was achieved by means of 13-tonnes smooth steel drum rollers (Fig. 23).

Based on a number of field density tests, including sand cone replacement and nuclear density techniques, it was concluded that 4 passes were adequate for attaining a fill density > 90% standard Proctor compaction. Dynamic cone penetration tests CPTs confirmed that compacted CW-BOS fills have greater strength compared to compacted sandy fill.

Fig. 23 Port Kembla construction site: during compaction [45].

Volumetric expansion was also measured for a period of about 180 days. Swelling was found to be substantial for both the blends. According to field trial and laboratory investigations, although the strength of CW-BOS blend with SFS content > 50% may be better compared to most conventional fills, such considerable level of swelling (i.e. > 3%) should be employed with caution for CW-SFS mixture when used as structural fill, unless the live load exceeds the swell pressure (about 100 kPa for BOS).

CONCLUSIONS

This keynote paper presents the geotechnical behaviour of granular materials in railway and port environment through results of large scale laboratory tests as well as the findings from full-scale instrumented tracks.

Main factors affecting ballast deformation such as ballast breakage and confining pressure were examined. The effects of particle breakage on the plastic distortional and volumetric strains were captured using constitutive model based on the critical state framework. By using a large-scale process simulation prismoidal traxial apparatus, the cyclic behaviour of granular layers was investigated. Ballast breakage was found to be influenced by the amount of lateral track confinement, frequency as well as type of loads (i.e. cyclic and impact). The plane strain condition was adopted to simulate in-situ track envinronment. Ballast stabilised with the geocomposite exhibited the least vertical deformation compared to ballast stabilized with geogrid and/or geotextile. Lateral spread reduction index (LSRI) was proposed to assess the deformations of geogrid-reinforced ballast. It was shown that LSRI is influenced by the type of geogrid. For geogrids placed at the subballast-ballast interface, the LSRI varies from 0.06 to 0.25. However, LSRI increases significantly and attains a maximum value of 0.37 for geogrid placed at 65 mm above the subballast. Both ballast breakage and associated settlements exhibited a significant reduction with the increase in LSRI.

Impact caused the most significant damage to ballast, especially under high repetitive loads, while just few impact blows caused considerable ballast damage. The shock mats could decrease impact induced strains in ballast by as much as 50%. The improved performance of sub-ballast was observed when used in conjunction with geocells. The geocell had a significant impact on the behaviour of sub-ballast at very low confining pressure ($\sigma'_3 \leq 15$ kPa) and higher frequency ($f \geq 10$ Hz). The resilient modulus of sub-ballast was substantially increased by utilizing geocell mattress as cellular confinement.

The results of the field study at Bulli indicated that the use of geocomposite as reinforcing elements for recycled ballasted tracks proved to be a feasible and effective alternative. The test results demonstrated that geocomposite was able to reduce the lateral deformation of fresh ballast by about 50% and recycled ballast by 10%. The results of the Singleton study showed that the effectiveness of the geosynthetic reinforcement increased as the subgrade decreased in stiffness. The geogrids with an optimum aperture size significantly reduced ballast deformations through improved interlock with the particles.

As an alternative to conventional freshly quarried or dredged sand fills, the potential use of CW and BOS as the predominant reclamation fill was examined for the 45 ha reclamation project at the Outer Harbor extension of Port Kembla, at Wollongong. Laboratory tests indicated there are

optimum CW-SFS mixtures that may meet most of the geotechnical specifications and which could be used as an effective structural fill.

The large-scale laboratory measurements and full-scale field monitoring have demonstrated improved performance of granular materials when (i) used in tandem with geosynthetic grids, geocells and shock mats in railways and (ii) used as an optimum mix in port environment.

ACKNOWLEDGEMENTS

The authors are grateful to the Australian Research Council for the funding of this research. The authors express their sincere thanks to Sydney Trains (previously RailCorp), Australian Rail Track Corporation (ARTC), Aurizon (previously Queensland Rail National), Queensland Main Roads, Port of Brisbane Corporation, Roads and Maritime Services (NSW), Coffey Geotechnics, Polyfabrics, Geofabrics, ARUP, Douglas Partners, Sydney Trains, ARTC, Chemstab, Austress Menard, Port Kembla Corporation, BHP-Billiton and ASMS among others.

The assistance of Mr David Christie (formerly Senior Geotechnical Consultant, RailCorp), Mr Tim Neville (ARTC), Mr Michael Martin (Aurizon), Mr Damien Foun (Aurizon), and Mr Sandy Pfeiffer (formerly Senior Geologist, RailCorp) is gratefully acknowledged. The authors would like to thank Mr Alan Grant (laboratory manager), Mr Cameron Neilson and Mr Ian Bridge (technical staff) at the University of Wollongong for their assistance throughout the period of this study. The on-site assistance provided by Mr David Williams of ARTC, Carol Bolam, Tony Miller, and Darren Mosman of Hunt8r Alliance (Newcastle) is much appreciated. A number of current and past doctoral students, including Dr Joanne Lackenby, Dr Wadud Salim, Dr Qideng Sun, Dr Mehdi Biabani, Dr Ali Tasalloti as well as former research academics, Dr Anisha Sachdeva (Project Manager, Huon Contractors Pty Ltd, Australia), Dr Pongpipat Anantanasakul (lecturer, Mahidol University Thailand) and Dr Gabriele Chiaro (lecturer, University of Canterbury, New Zealand) have all contributed to the contents of this paper.

This Keynote paper can be considered as a significant extension of the 2012 Australian Heritage Lecture at the International Conference on Ground Improvement and Ground Control delivered by the 1st author. A significant portion of the contents have been reproduced with kind permission from the Journal of Geotechnical and Geoenvironmental Engineering ASCE, International Journal of Geomechanics, ASCE, ASTM Geotechnical Testing Journal, Géotechnique, and Canadian Geotechnical Journal, among others. Some salient contents of these past articles have been reproduced with kind permission from the original sources.

REFERENCES

1. Marsal, R.J. (1973), Mechanical properties of rock fill. In: Hirschfield R.C. and Pools, S.J. (eds) *Embankment Dam Engineering*: Casagrande Volume, Wiley, New York, 109-200.
2. Indraratna, B., Lackenby, J. and Christie, D. (2005), Effect of confining pressure on the degradation of ballast under cyclic loading, *Géotechnique*, 55(4), 325-328.
3. Lackenby, J., Indraratna, B., McDowell, G. and Christie, D. (2007), Effect of confining pressure on ballast degradation and deformation under cyclic triaxial loading, *Géotechnique*, 57(6), 527-536.
4. Nimbalkar, S., Indraratna, B., Dash, S.K. and Christie, D. (2012), Improved performance of railway ballast under impact loads using shock mats, *Jl. of Geotech. and Geoenv. Engineering, ASCE*, 138(3), 281-294.
5. Lim, W.L., McDowell, G.R. and Collop, A.C. (2004), The application of Weibull statistics to the strength of railway ballast, *Granular Matter*, 6(4), 229-237.
6. Indraratna, B., Khabbaz, H., Salim, W., Lackenby, J. and Christie, D. (2004), Ballast characteristics and the effects of geosynthetics on rail track deformation, *Int. Conference on Geosynthetics and Geoenvironmental Engineering*, Mumbai, India, 3-12.
7. Sun, Y., Indraratna, B., and Nimbalkar, S. (2014), Three-dimensional characterisation of

particle size and shape for ballast, *Géotechnique Letters*, 4(3), 197-202.
8. Le Pen, L., Powrie, W., Zervos, A., Ahmed, S. and Aingaran, S. (2013), Dependence of shape on particle size for a crushed rock railway ballast, *Granular Matter*, 15(6), 849-861.
9. Raymond, G.P. (2002), Reinforced ballast behaviour subjected to repeated load, *Geotextiles and Geomembranes*, 20(1), 39-61.
10. Shin E.C., Kim, D.H. and Das, B.M. (2002), Geogrid-reinforced railroad bed settlement due to cyclic load, *Geotechnical and Geological Engineering*, 20(3), 261-271.
11. Indraratna, B. and Salim, W. (2003), Deformation and degradation mechanics of recycled ballast stabilised with geosynthetics, *Soils and Foundations*, 43(4), 35-46.
12. Indraratna, B., Khabbaz, H., Salim, W. and Christie, D. (2006), Geotechnical properties of ballast and the role of geosynthetics in rail track stabilization, *Proceedings of the ICE - Ground Improvement*, 10(3), 91-101.
13. Indraratna, B., Shahin, M.A. and Salim, W. (2007), Stabilising granular media and formation soil using geosynthetics with special reference to Railway engineering, *Proceedings of the ICE - Ground Improvement*, 11(1), 27-44.
14. Li, D., and Selig, E. T. (1998), Method for railroad track foundation design. I: Development. *Jl. of Geotech. and Geoenv. Engineering, ASCE*, 124(4), 316-322.
15. Indraratna, B. and Nimbalkar, S. (2013), Stress-strain-degradation response of railway ballast stabilised with geosynthetics, *Jl. of Geotech. and Geoenv. Engineering, ASCE*, 139(5), 684-700.
16. Indraratna, B., Hussaini, S.K. and Vinod, J.S. (2013), The lateral displacement response of geogrid-reinforced ballast under cyclic loading, *Geotextiles and Geomembranes*, 39, 20-29.
17. Ashpiz, E.S., Diederich, R., and Koslowski, C. (2002), The use of spunbonded geotextile in railway track renewal St Petersberg-Moscow, *7th Intl. Conf. on Geosynthetics*, Nice, France, 1173-1176.
18. Indraratna B., Nimbalkar, S. and Christie, D. (2009), The Performance of Rail Track Incorporating the Effects of Ballast Breakage, Confining Pressure and Geosynthetic Reinforcement, *8th Intl. Conf. on the Bearing Capacity of Roads, Railways, and Airfields*, London: Taylor and Francis Group, 5-24.
19. Indraratna, B., Nimbalkar, S., Christie, D., Rujikiatkamjorn, C. and Vinod, J.S. (2010), Field assessment of the performance of a ballasted rail track with and without geosynthetics, *Jl. of Geotech. and Geoenv. Engineering, ASCE*, 136(7), 907-917.
20. Indraratna, B., Nimbalkar, S. and Rujikiatkamjorn, C. (2014), Enhancement of Rail Track Performance through Utilisation of Geosynthetic Inclusions, *Geotech. Eng. Jl. of the SEAGS & AGSSEA*, 45(1), 17-27.
21. Indraratna, B., Nimbalkar, S., and Neville, T. (2014), Performance assessment of reinforced ballasted rail track, *Proceedings of the ICE - Ground Improvement*, 167 (1), 24-34.
22. Indraratna, B., Nimbalkar, S., and Rujikiatkamjorn, C. (2014), From theory to practice in track geomechanics - Australian perspective for synthetic inclusions. *Transportation Geotechnics J.*, 1(4), 171-187.
23. Brown, S.F., Kwan, J. and Thom, N.H. (2007), Identifying the key parameters that influence geogrid reinforcement of railway ballast, *Geotextiles and Geomembranes*, 25(6), 326-335.
24. Indraratna, B., Hussaini, S.K. and Vinod, J.S. (2012), On the shear behavior of ballast-geosynthetic interfaces, *ASTM Geotech. Testing Jl.*, 35(2), 305-312.
25. Dash, S.K., Krishnaswamy, N.R. and Rajagopal, K. (2007), Behaviour of geocell-reinforced sand beds under strip loading, *Canadian Geotechnical Journal*, 44(7), 905-916.
26. Hegde, A.M. and Sitharam, T.G. (2014), Effect of infill materials on the performance of geocell reinforced soft clay beds, *Geomechanics and Geoengineering*, 1-11.
27. Yang, X., Han, J., Pokharel, S.K., Manandhar, C., Parsons, R.L., Leshchinsky, D. and Halahmi, I. (2012), Accelerated pavement testing of unpaved roads with geocell-reinforced sand bases, *Geotextiles and Geomembranes*, 32(6), 95-103.

28. Tafreshi, S.N.M., Khalaj, O. and Dawson, A. R. (2014), Repeated loading of soil containing granulated rubber and multiple geocell layers, *Geotextiles and Geomembranes*, 42(1), 25-38.
29. Leshchinsky, B., and Ling, H. (2013), Effects of geocell confinement on strength and deformation behavior of gravel, *Jl. of Geotech. and Geoenv. Engineering, ASCE*, 139(2), 340-352.
30. Indraratna, B., Biabani, M.M. and Nimbalkar, S. (2015), Behavior of geocell reinforced subballast subjected to cyclic loading in plane strain condition, *Jl. of Geotech. and Geoenv. Engineering, ASCE*, 141(1), 04014081.
31. Indraratna, B., Nutalaya, P., Koo, K.S. and Kuganenthira, N. (1991), Engineering behavior of low carbon, pozzolanic fly ash and its potential as a construction fill, *Can. Geotech. J.*, 28(4), 542-555.
32. Lim, T. and Chu, J. (2006), Assessment of use of spent copper slag for land reclamation, *Waste Management Research*, 24(1), 67-73.
33. Türkel S. (2006), Long-term compressive strength and some other properties of controlled low strength materials made with pozzolanic cement and Class C fly ash, *J Hazard Mater.*, 137(1), 261-266.
34. Raymond, G.P. (1979), Railroad Ballast Prescription: State-of-the-Art, *Jl. of Geotech. Engineering Div., ASCE*, 105(GT2), 305-322.
35. Salim, W. and Indraratna, B. (2004), A new elasto-plastic constitutive model for granular aggregates incorporating particle breakage, *Canadian Geotechnical Journal*, 41, 657-671.
36. Jeffs, T., and Tew, G.P. (1991), A review of track design procedures: *sleepers and ballast, Vol. 2*, Railways of Australia BHP Research, Melbourne Laboratories, Melbourne, Australia.
37. Sun, Q.D., Indraratna, B. and Nimbalkar, S. (2014), Effect of cyclic loading frequency on the permanent deformation and degradation of railway ballast, *Géotechnique*, 64(9), 746-751.
38. Sun, Q.D., Indraratna, B. and Nimbalkar, S. (2015), The deformation and degradation mechanisms of railway ballast under high frequency cyclic loading, *Jl. of Geotech. and Geoenv. Engineering, ASCE*, 10.1061/(ASCE)GT.1943-5606.0001375.
39. Indraratna, B., Nimbalkar, S. and Tennakoon, N. (2010), The behaviour of ballasted track foundations: track drainage and geosynthetic reinforcement, *ASCE Annual GI Conf. GeoFlorida 2010*, Florida, USA, 2378-2387.
40. Standards Australia. (1996), Aggregates and rock for engineering purposes, Part 7: Railway ballast AS 2758.7-1996. Sydney, NSW, Australia.
41. Indraratna, B., S. Nimbalkar and C. Rujikiatkamjorn (2012), Track Stabilisation with Geosynthetics and Geodrains, and Performance Verification through Field Monitoring and Numerical Modelling, *Int. J. of Railway Technology*, 1(1), 195-219.
42. Indraratna, B., Nimbalkar, S. and Rujikiatkamjorn, C. (2014), Modernisation of rail tracks for higher speeds and greater freight, *Int. J. of Railway Technology*, 2(3), 1-20.
43. Shin E.C., Kim D.H. and Das B.M. (2002), Geogrid-reinforced railroad bed settlement due to cyclic load, *Geotechnical and Geological Engineering*, 20(3), 261-271.
44. Indraratna, B., Sun, Q.D. and Nimbalkar, S. (2014), Observed and predicted behaviour of rail ballast under monotonic loading capturing particle breakage. *Canadian Geotech. J.*, 52(1), 73-86.
45. Indraratna, B. (2012), Ground improvement for transportation infrastructure in Australia. *Proc. Int. Conf. on Ground Improvement and Ground Control*, Wollongong, Australia, 131-150.
46. Chiaro, G., Indraratna, B., Tasalloti S.M.A., Rujikiatkamjorn, C. (2015), Optimisation of coal wash-slag blend as a structural fill. *Proceedings of the ICE - Ground Improvement*, 168(1), 33-44.